

IUP: An Intelligent Utility Prediction Scheme for Solid-State Fermentation in 5G IoT

Min Wang, Shanchen Pang, Tong Ding, Sibao Qiao, Xue Zhai, Shuo Wang, Neal N. Xiong *Senior Member, IEEE*, Zhengwen Huang

Abstract—At present, SOLID-STATE Fermentation (SSF) is mainly controlled by artificial experience, and the product quality and yield are not stable. Accurately predicting the quality and yield of SSF is of great significance for improving human food security and supply. In this paper, we propose an Intelligent Utility Prediction (IUP) scheme for SSF in 5G Industrial Internet of Things (IoT), including parameter collection and utility prediction of SSF process. This IUP scheme is based on the environmental perception and intelligent learning algorithms of the 5G Industrial IoT. We build a workflow model based on rewritable petri net to verify the correctness of the system model function and process. In addition, we design a utility prediction model for SSF based on the Generative Adversarial Networks (GAN) and Fully Connected Neural Network (FCNN). We design a GAN with constraint of mean square error (MSE-GAN) to solve the problem of few-shot learning of SSF, and then combine with the FCNN to realize the utility prediction (usually use the alcohol) of SSF. Based on the production of liquor in laboratory, the experiments show that the proposed method is more accurate than the other prediction methods in the utility prediction of SSF, and provide the basis for the numerical analysis of the proportion of preconfigured raw materials and the appropriate setting of cellar temperature.

Index Terms—solid-state fermentation, utility prediction, petri net, mean square error

1 INTRODUCTION

SOLID-STATE fermentation (SSF) has been defined as the fermentation process which involves solid matrix and is carried out in absence or near absence of free water [1]. The purpose of SSF is to accumulate the target metabolites. SSF takes a certain proportion of raw materials and an appropriate cellar-entry temperature as the main preconditions for cellar-entry fermentation [2]. Once the raw material was sent into the fermentation cellar, no operation can be applied to the fermentation cellar until the end of fermentation. The yield and quality of SSF always instability by traditional method which depends on artificial expertise to control the proportion of raw materials. The relationship between raw material parameters should be analyzed. The 5G Internet of Things (IoT) is one of the technologies to realize industrial mass production, which provide the method to collect the parameters [3]. Therefore, the traditional industry of SSF should be further enhanced with the technology of 5G IoT to realize the intelligent manufacturing of SSF industry. The production process of Chinese liquor is a typical SSF [4]. We study the utility prediction of the fermentation process of Chinese liquor, which provide a method to predict the yield and quality of SSF.

Now, changing raw materials and adjusting cellar temperature are the two main method to improve the Chinese liquor product quality and yield of SSF. [5] analyzes the influence of different raw materials on the quality but the effects of different proportions of materials on liquor quality is not studied. Microbial is another factors which affect the quality of SSF. [6][7] research the quality of liquor of different microbial community. The main microorganisms affecting the quality of rice-liquor were analyzed in [8], and the optimum temperature of the microorganism was studied. Changes in the temperature of the grains in the fermentation cellar will have a significant impact on the growth and metabolism of microorganisms, which in turn will affect the yield and quality of liquor [9][10]. In [11], authors research the influence of the temperature trend in the fermentation cellar on the yield and quality of liquor, and it is concluded that the temperature curve of high-quality liquor should be with the trend of rise slowly in the early stage, rise rapidly in the middle stage and drop slowly in the later stage.

Nevertheless, different liquors have different microbial communities. The microorganism through biological experiments, especial the impact of microbes on the liquor SSF is a essential research field. At the same time, the research of real-time monitoring and control of the fermentation temperature ignores that fermentation cellar cannot be opened during the SSF process. In order to improve the yield and quality of all liquors without controlling the fermentation process, another effective method is to control the key preconditions of SSF in advance, because the proportion of preconditions is a vital factor affecting the quality and yield of SSF products [11].

It is a technical approach that improve the utility of SSF by optimizing the key cellar entry preconditions. IoT

- M. Wang is with Department of Control Science and Engineering, China University of Petroleum, Qingdao 266580, China. E-mail: min-wang2020@qq.com.
- S. Pang, S. Qiao and X. Zhai are with Department of Computer Science and Technology, China University of Petroleum, Qingdao 266580, China. E-mail: pangsc@upc.edu.cn, 1175928825@qq.com.
- T. Ding is with school of software, Shandong University, China. E-mail: 793394086@qq.com.
- Neal N. Xiong is with Department of Mathematics and Computer Science Northeastern State University, Tahlequah, OK, USA. E-mail: xionгнаixue@gmail.com, xiong31@nsuok.edu.
- S. Wang is Department of Computer Science and Technology, Tongji University. E-mail: 8362084547@qq.com.

provides the necessary methods for collecting parameters such as liquor Alcohol, Temperature, humidity, Starch content, and Acidity in the SSF process. These parameters provide the data analysis samples for the optimization of key cellar-entry preconditions of SSF. Parameters collection and prediction system of SSF of Chinese liquor based on 5G Industrial IoT is shown in Fig. 1. The system analytical model based on the 5G Industrial IoT established in this paper plays a key role in analyzing the mathematical relationship between parameters and predicting the quality and yield of products correctly. Moreover, it is necessary to verify correctness of the model.

Since the parameters of SSF process are obtained by regular or irregular collection, which is a typical dynamic discrete event, and the collection times of parameter samples are dynamic. Hence, the system model needs reconstruction in the collection structure. Petri net is a graphic modeling tool with a strict mathematical definition and is well applied to describe the process such as discrete, synchronous, asynchronous, and concurrent processes [12]. Rewritable Petri nets [13] was proposed to solve the formal description and modeling in dynamic system reconstruction. Rewritable Petri nets provide a better analysis and verification method for dynamic discrete systems [14][15] with structural reconstruction. Therefore, the rewritable petri net can be well applied to model and verify the system model of the parameter collection and analysis of SSF. To predict the quality and yield of SSF, we use deep learning to analysis the hidden relationship between parameters. Neural network training needs numerous data. More sufficient data make the relationship mining more accurate, which leads to more ways to generate more data.

In this work, Our main contributions are as follows:

- To establish an IUP framework of SSF of Chinese liquor based on deep learning.
- To guarantee the correctness of the framework, we propose an edge-rewritable petri net to model and verify the soundness of the system.
- To realize the learning parameter relationship in the system model, we design an MSE-GAN model to expand the parameters of SSF process and analyze the relationship between these parameters of SSF process by using fully connected neural network.

The rest of this work is arranged as follows: the related works are introduced in Section II. Section III introduces the system framework and builds the rewritable petri net model of the system framework, and analyzes the soundness of the model. Section IV describes the algorithm of MSE-GAN and the utility prediction model of SSF based on fully connected neural network. Section V verifies our method and experiments. The last Section summarizes the work of the paper and future work.

2 RELATED WORK

The main raw material of SSF is grain. In 2019, the consumption of grain in the wine industry by SSF reached 30 million tons. The sauce, vinegar and other products in our daily life are all products of SSF. According to statistics, about 10%-15% of grain is converted into food necessities through SSF. This year, the impact of COVID-19 given high priority

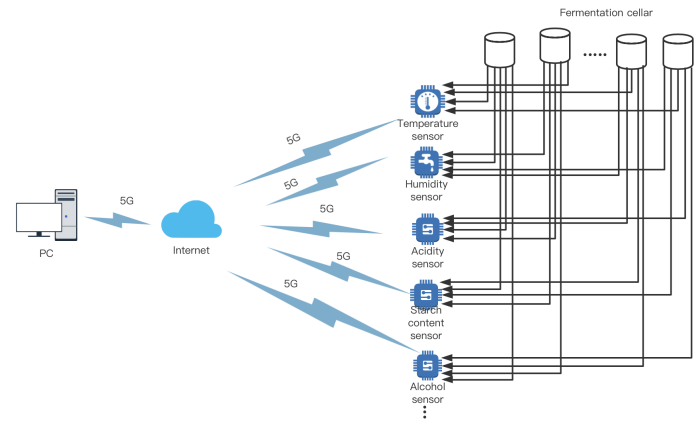


Fig. 1. The collection and prediction system of SSF process of Chinese liquor based on Internet of things.

to food security, leading to the worst global food crisis in 50 years. Therefore, it is of great significance to predict the fermentation environment, establish the best SSF environment, and improve the yield and quality of SSF to ensure the national food security. At present, many researches focus on improving the quality and yield of SSF. In [42], the use of oilseed as the substrate for SSF can improve the content of unsaturated fatty acids and protein in the products. In [43], microorganisms are used to improve the production process of SSF, which can increase the yield of SSF and shorten the time of SSF process. Authors in [44] Response Surface Methodology (RSM) to optimize the parameters of SSF such as time, pH and temperature can enhance the production of alginate

The SSF is mainly optimized by microorganisms. However, each product of SSF needs to be analyzed because different raw materials use different microorganisms. As a result, microbial optimization of SSF is not universal. The intelligent production of SSF industry is realized by using IoT. The industrial IoT mainly uses sensor [45][46] technology to collect data in the industrial production process. In order to solve the security problem of industrial control system, Zhang et al [6] design a dynamic network security risk assessment method, which can assess the risk caused by unknown attacks. Authors in [47] develop a new security design using MODBUS protocol to provide higher security guarantee for IT infrastructure. Yang et al [48] design a robot obstacle avoidance algorithm, which is effectively applied in industrial automation production. In order to realize the efficient production in SSF industry, it is necessary to collect the data of the SSF process through the sensor in real time to analyze the relationship between the data by using the deep learning method. This will improve the yield and quality of the SSF.

The process of IUP of SSF is a workflow. It is necessary to model the workflow to ensure the correctness of it. The traditional workflow models include the Event-Condition-Action (ECA), Business Process Execution Language (BPEL) and Yet Another Workflow Language (YAWL). These modeling approaches describe business process as a set of activities executed by a fixed control flow. In [31], An object-centered modeling method is proposed, which defines three

abstract types of business objects responsible for creating and managing tasks and subprocesses, and modeling the life cycle of business objects by using gateway Extended Finite State Machine (FSM). However, the model constructed by the modeling method need to be converted to YAWL model and performed in YAWL engine [32]. Lin et al. [33] model the serverless applications, predict the average end-to-end response time and workflow cost through the model to realize the optimal configuration of serverless applications. However, these model do not scale well and have some limitations when modeling dynamic systems. Petri net is a model developed to describe distributed system. In [30], authors use the petri net to model the application over the heterogeneous clouds to manage these applications. In [13], the authors propose a place rewritable petri net which can be used to model the reconfiguration systems. According to the process of collecting the parameters of SSF process, we propose the edge-rewritable petri net to model the SSF process system.

The data generated from the process of SSF is in one-dimensional format. We need to generate more effect data when the collected data is not sufficient. Generative Adversarial Networks (GAN) was proposed by Goodfellow in [18], which can generate effective data by using few-shot data. GAN is not relay on any prior assumptions in data generation. It makes the generated data conform to the distribution of actual data through the game between Generator (G) and Discriminator (D). The G network receives a random noise z , and generates data of approximate samples as much as possible. The D network receives an input data and tries to discriminate whether the data is a real sample or a fake sample generated by the network.

Now, GAN is widely applied in the image data generation [19], voice data generation [20], text data generation [21], etc. The image data augmentation method of pedestrians of small scale or in heavy occlusions is proposed in [25], the image generated in this paper holds good visual quality as well as attributes. In [26], authors repair the aging image, the original image data is supplemented by GAN, and the high-quality image is generated. The image data is mainly stored in the form of matrix. For the generation of one-dimensional data, the storage mode of data should be converted. In [34], a Classification enhancement GAN is proposed to solve the problem of data imbalance in classification, which enhance the accuracy of target prediction in the case of data imbalance. Liu et al. [35] propose an Adversarial Symmetric GANs (AS-GANs) which combines the training to real samples by D network with ordinary GAN. It makes the adversarial training become symmetry, stable training and accelerate the convergence. Yin et al. [36] introduce the time series into GAN, which can effectively solve the problem of disharmony between intelligent generation control and generation command scheduling. In view of the successful application of GAN in image data processing, we apply GAN to the production of one-dimensional data.

After obtaining more valid data, the relationship between different attribute data needs to be analyzed. Bayesian network (BN) models and the Markov model (MM) are two even prediction model. However, the prediction of these two methods mainly depends on the latest

state. These methods can be used for reasoning and calculation, but the whole process is oversimplified and the important characteristics of many state nodes are ignored, resulting in low accuracy of prediction. FCNN is a computational model that imitates biological neural network [22], it has three parts: input layer, hidden layer and output layer. FCNN is a modeling technology of deep learning and is widely used in the field of classification, prediction etc. In [27], authors calculate the tilt misalignments of the off-axis telescope by FCNN. In [28], this paper classify radar clutter and real radar target by using the FCNN. [29] solves the accurate classification of the arrhythmia by a dual FCNN.

FCNN has a number of research achievements in the field of prediction. In the [23], authors use the LSTM to simulate the local variation of PM2.5 pollution and then use FCNN to predict the air quality. The FCNN is used to predict and identify the arc faults in [24]. In [29], authors use the FCNN to predict the environmental factors of landslide susceptibility. A global-to-local localization approach using FCNN is proposed in [37] to localize anatomical landmarks in medical images. In [38], The combination of FCNN and two LSTM components can effectively predict train delays caused by weather and other conditions. The FCNN is combined with VGG19 in [39], which covers the multiple scale features. As a result, it can effectively predict the degree of cancer lesions. Wang et al., [40] found that FCNN could measure the conditional correlation between genes by using the similarity of co-expression and prior knowledge, and the experiment proved that FCNN could effectively predict the genetic relationship. Ale et al. [41] uses FCNN to learn and predict BRNN, which realizes the prediction of active cache of edge computing to relieve the pressure of core network in the Internet of Things. Based on these researches about the FCNN, FCNN can be well applied in analyzing and predicting data, so we adopt the FCNN to predict the quality and yield of SSF.

3 SYSTEM MODEL OF REWRITABLE PETRI NET

In order to guarantee the correctness of the system framework of IUP of SSF. This Section employs the edge-rewritable petri net to model and illustrate the correctness of the system framework.

3.1 System Framework

The system framework include parameter collection of SSF process and study the relationship between parameters. The main parameters in SSF of Chinese liquor include the acidity, starch content, humidity, maternal draff, Daqu, bran shell, original cellar temperature and ground temperature. These parameters affect the cellar temperature and the quality and yield of liquor. The factors of acidity, starch content, humidity, maternal draff, Daqu, bran shell affect each other in pairs. In order to obtain the mathematical relationship between these parameters and realize the intellectualization of liquor industry, this paper combines the SSF industry with deep learning to realize the utility prediction of SSF. The system framework diagram is shown in Fig. 2.

Step1: parameters will be collected several times by the sensor.

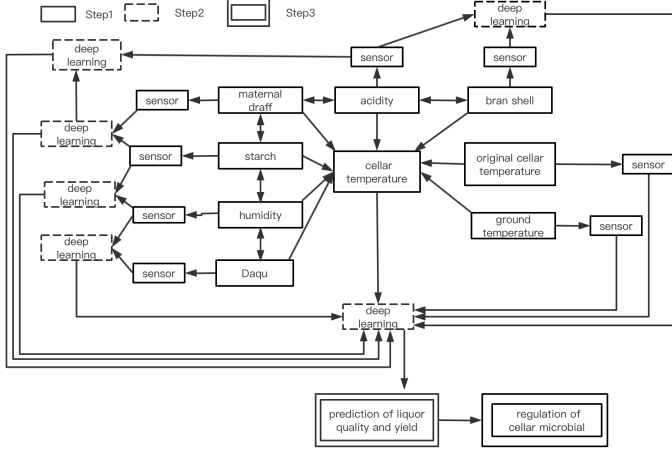


Fig. 2. The system framework of IUP of SSF.

Step2: the relationship between parameters will be studied by deep learning.

Step3: the utility prediction model of SSF are obtained.

The utility prediction model provides a basis for the numerical analysis of the preconditions of SSF and provides a guidance for the regulation of microbial community, so as to optimize the liquor production.

3.2 Edge Rewritable Petri Net

Petri net is a workflow modeling and analysis tool. According to the characteristic that the parameters of SSF process need to be collected several times, the rewritable Petri net is proposed to model the framework.

Definition 1 (petri net[13]) The 4-tuple $N = (P, T, F, M_0)$ is called a Petri net, where P is a set of places. Each place have several tokens, whose length of tuples is determinate. T is a finite set of transition. $P \cap T = \emptyset$. Iff 3-tuple (P, T, F) is a net. $F \subseteq (P \times T) \cup (T \times P)$ is a set of arcs. A marking of N is a function $M: P \rightarrow \mathbb{N}$. M_0 is an initial marking, $\mathbb{N} = \{0, 1, 2, \dots\}$ is a set of non-negative integer.

(1) $\cdot x = \{y \mid (y, x) \in F\}$ is a input set or preset of x . And $x \cdot = \{y \mid (y, x) \in F\}$ is called output set or post-set of x .

(2) $\forall M_1$ and $M_2, M_1 \leq M_2$, if and only if for all $p \in P: M_1(p) \leq M_2(p)$.

Then the firing rule of N is introduced as follows:

(3) Transition $t \in T$ is enabled in a marking M , iff $\forall p \in \cdot t, M(p) \geq 1$, which is denoted as $M[t]$.

(4) If transition $t \in T$ is enabled in a marking M , the t can be fired and generate a new marking M' , which is denoted as $M[t]M'$:

$$M' = \begin{cases} M(p) - 1, & p \in \cdot t - t; \\ M(p) + 1, & p \in t - \cdot t; \\ M(p), & \text{other.} \end{cases}$$

Suppose that $R(M_0)$ represents all marking set, which N can reach from M_0 . If $\exists M_1, M_2, \dots, M_k \in R(M_0)$ and $\forall i: 1 \leq i \leq k, \exists t_i \in T: M_i[t_i]M_{i+1}$, the transition sequence $\sigma = t_1 t_2 \dots t_k$ is enabled in a marking M_1, M_{k+1} is reachable from M_1 , which is denoted as $M_1[\sigma]M_{k+1}$.

Definition 2 (edge rewritable petri nets) A 7-tuple $EN = (P, T, F, K, W, M, W_v)$ is an edge rewritable petri net, where (P, T, F) is a basic petri net:

(1) $W: F \rightarrow \{0, 1, 2, \dots\}$ is a weight function, $K: S \rightarrow \{0, 1, 2, \dots\}$ is a capacity function, $M: P \rightarrow \{0, 1, 2, \dots\}$ is a marking function of EN and satisfy the condition of $\forall p \in P: M(s) \leq K(s)$.

(2) The firing rules of transition t in EN is introduced as follows:

$$\begin{cases} M(p) \geq W(p, t), & p \in \cdot t - t; \\ M(p) + W(p, t) \geq K(p), & p \in t - \cdot t; \\ M(p) - W(p, t) + W(t, p) \geq K(p), & p \in \cdot t \cap t. \end{cases}$$

If transition $t \in T$ is enabled in a marking M , the t can be fired and generate a new marking M' , which is denoted as $M[t]M'$:

$$M' = \begin{cases} M(p) - W(p, t), & p \in \cdot t - t; \\ M(p) + W(p, t), & p \in t - \cdot t; \\ M(p) - W(p, t) + W(t, p), & p \in \cdot t \cap t; \\ M(p), & \text{other.} \end{cases}$$

(3) $\exists f \in F$ is an rewritable edge, when $t_i \in T$ and t_i is a vertex of f , $\#(t_i/\sigma) = W_v \rightarrow F = F - \{f\}$. $W_v \in \mathbb{N}^*$ is the rewritable restriction of f . σ is a sequence of transitions, $\#(t_i/\sigma)$ denotes the number of t_i occurrence in σ . The rewritable edges are represented by dashed lines.

Definition 3 $N = (P, T, F)$ is a workflow[23] where

(1) If N has two special places start and end that $\cdot \text{start} = \emptyset$, $\text{start} \cdot = \emptyset$.

(2) N is an extended workflow with a new transition t that $\cdot t = \{\text{start}\}$ and $t \cdot = \{\text{end}\}$. This extended workflow is strongly connected.

3.3 The rewritable petri net model of the system framework

To analysis the relationship between the raw materials parameters and alcohol. We use the edge-rewritable petri net to model the framework. The place P denotes parameters and relation models of parameters, meanwhile, the transition T denotes the operation of collecting and studying the parameters relationships. The rewritable edges can realize the multiple collecting parameters.

According to the system framework, we use the rewritable petri net to model the system framework for IUP of SSF. Capital letters are used to indicate the parameters of Chinese liquor SSF. **M**: master grains, **S**: starch content, **D**: Daqu, **H**: humidity, **A**: acidity, **B**: bran shell, **C**: cellar temperature, **G**: ground temperature, **ALC**: alcohol. The rewritable petri net model of the system framework is shown in Fig. 3. The meaning of all the elements in Fig. 3 are shown in Table I and Table II.

In this model, P_{start} is a start place with a token, transition t_0 denotes the operation of taking materials into the cellar. First, t_0 can be fired and these parameters places $P_B, P_A, P_M, P_S, P_H, P_D, P_C, P_G, P_{ALC}$ obtain a token. Now, the collected transition of $t_1, t_2, t_3, t_4, t_5, t_6, t_7, t_8, t_9$ can be fired. If t_1 was fired, then the collected parameter place P_{B1} will get a token which means the parameter of B is obtained, meanwhile, P_B also get a token and transition t_1 will be fired again. t_1 was fired several times, which is a loop structure represents the process of collecting data several times. When the amount of stimulation of t_1 is equal to W_{v1} , the rewritable edge $f = (t_1, P_B)$ will disappear. Naturally, when transition t_2 was fired, the acidity collecting parameter

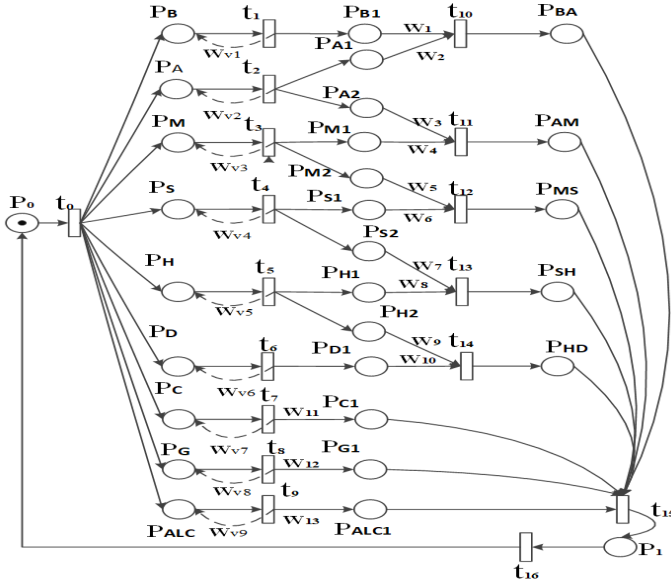


Fig. 3. A rewritable petri net model of the system framework.

places of P_{A1} and P_{A2} will get a token respectively at the same time. In addition, the acidity parameter place P_A also get a token and transition t_2 will be fired again. When the times that t_2 was fired is equal to W_{v2} , the rewritable edge $f=(t_2, P_A)$ will disappear. If the number of tokens in P_{B1} and P_{A1} is equal to weight function W_1 and W_2 respectively, then the study transition t_{10} will be fired. Next, the place P_{BA} of relation model for parameter B and A will get a token. When the collect transition t_3 was fired, places P_{M1} , P_{M21} will get a token respectively. Once t_3 is fired and the amount of stimulation is equal to the rewritable constraint W_{v3} , the rewritable edge $f=(t_3, P_M)$ will disappear. If the collection times is equal to the limitation of the weight function W_{v4} , the collecting parameter place P_{M1} will get the amount of tokens of W_{v4} , at the same time, if the place P_{A2} also get the amount of tokens of W_{v3} , then the study transition of t_{11} can be fired and the relation model place P_{AM} of parameter A and M will obtain a token. Similarly, the study transition of t_{12} , t_{13} and t_{14} are fired in the same way. Finally, we acquire the prediction model of liquor quality and yield. At this time, the workflow model of the system framework is completed. In addition, we add an adjust transition t_{16} and the edges of (P_1, t_{16}) and (t_{16}, P_{start}) form an extended network which can be used to readjust the precondition parameters **B**, **A**, **M**, etc.

3.4 The soundness of the system model

The soundness of the system model guarantee the correctness of the logics of the system framework. If a petri net is soundness, it will satisfy the following definition.

Definition 4 (boundedness [16]) A 7-tuple $EN=(P, T, F, K, W, M, W_v)$ is an edge rewritable petri net, where M_0 is the initial marking. If $\exists B \in \mathbb{N}^*$ and $\forall M \in R(M_0): M_p \leq B$, the place p is bounded. The minimum B is the bound of place p, which is denoted as $B(p)$. If each $p \in P$ in the net is bounded, EN is a bounded petri net.

$$B(p)=\min\{B \mid \forall M \in R(M_0): M(p) \leq B\}$$

TABLE 1
The meaning of each place in Fig. 3

Places	Meaning
P_{start}	Start
P_B, P_A, P_M, P_S	The parameter of Bran shell quality, Acidity, Maternal draff quality and Starch quality respectively.
$P_H, P_D, P_C, P_G, P_{ALC}$	The parameter of Humidity, Daqu quality, the Cellar-temperature, Ground temperature, ALCclcohol concentration respectively.
$P_{B1}, P_{C1}, P_{G1}, P_{ALC1}$	The collected parameter of Bran shell quality, the original Cellar-temperature, ground temperature, alcohol concentration respectively.
P_{A1}, P_{A2}	The collected parameter of Acidity
P_{M1}, P_{M2}	The collected parameter of Maternal draff
P_{S1}, P_{S2}	The collected parameter of Starch quality
P_{D1}, P_{D2}	The collected parameter of Humidity
P_{BA}	The relational model of Bran shell quality and Acidity
P_{AM}	The relational model of Acidity and Maternal draff quality
P_{MS}	The relational model of Maternal draff quality and Starch quality
P_{SH}	The relational model of Starch quality and Humidity
P_{HD}	The relational model of Humidity and Daqu quality
P_1	The relationship model of quality and yield of ALCclcohol

TABLE 2
The meaning of each transition and weight function in Fig. 3

T	Meaning	W	meaning
t_0	Into the cellar	$W_{v1} - W_{v9}$	The weight function of rewriteable edge
$t_1 - t_9$	collect	$W_1 - W_{10}$	The weight function
$t_{10} - t_{15}$	study		
t_{16}	adjust		

Definition 5 (liveness [16]) The edge rewritable petri net $EN=(P, T, F, K, W, M, W_v)$, if $t \in T$ and $\forall M \in R(M_0), \exists M'[t]$, the transition t is liveness. If $\forall t \in T$ is liveness, the edge rewritable petri net EN is liveness.

Definition 6 (soundness [16]) $EN=(P, T, F, K, W, M, W_v)$ is soundness if the following conditions hold:

(1) For each marking M which is reached by the start marking M_0 (the initial place p_{start} contains a token), there have transition sequence σ_1 and σ_2 that the end marking M_{end} reached from marking M, that is $\forall M: M_0[\sigma_1] M \rightarrow M[\sigma_2] M_{end}$.

(2) The end marking M_{end} (the end place p_{end} contains a token) is reachable from M and M_{end} is the only one end marking, that is $\forall M: (M_0[\sigma] M \cap M \geq M_{end}) \rightarrow (M=M_{end})$.

(3) There is no dead marking (Marking M can not be changed) in EN , that is $\forall t \in T, \exists M$ and M' have $M_0[\sigma] M [t] M'$.

Theorem 1 The edge rewritable petri net EN is soundness if the extended workflow [17] of EN is liveness and boundedness[16].

Reachability graph is a main tool to analysis the petri nets[16], which can be used to analyzed the boundness and liveness of petri net. Each point is a making in the reachability graph. We use the analysis software of petri net to build the reachability graph for the system rewritable petri net model. The result is that the reachability graph

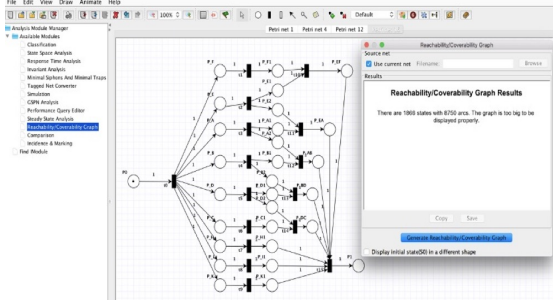


Fig. 4. The analysis of reachability graph of the rewritable petri net model of system framework

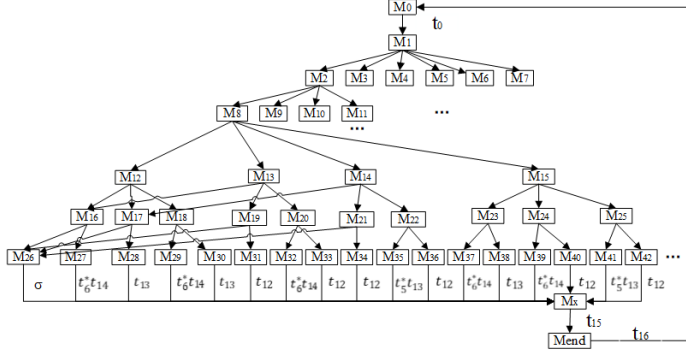


Fig. 5. The compressed reachability graph of the rewritable petri net model of system framework

includes 1866 reachability status and 8750 arcs. However, this reachability graph is too huge to show visually, and the result of analysis software is shown in Fig. 4. Naturally, the reachability graph need to be compressed, which satisfy the principle that the paths are not lost.

Definition 7 (Homogenous sequence) σ_1 and σ_2 are the transition sequences, if $M \xrightarrow{\sigma_1} M'$, $M \xrightarrow{\sigma_2} M'$, $\forall t \in \sigma_1 \wedge \forall t \in \sigma_2 \rightarrow \#(t/\sigma_1) = \#(t/\sigma_2)$, then σ_1 and σ_2 are the homogenous sequence. Using (σ_1) or (σ_2) to represent homogenous sequence, and $\#(t/\sigma_1)$, $\#(t/\sigma_2)$ denote the number of occurrences of transition t in σ_1 and σ_2 .

Property 1: According to definition 3, Two homogenous sequence start from the same marking M and reaches to another equal marking M' through different transition sequences. So, the paths between M and M' can be compressed, and the reachability of the original reachability graph remains unchanged after compression.

We compress the reachability graph of the system rewritable petri nets model according to the principle of homogeneous sequence compression. Because of the transition $t_1, t_2, t_3, t_4, t_5, t_6, t_7, t_8, t_9$ will be fired for many times according to the collection times in the system rewritable petri nets model. Using t_i^* denotes the transition sequence $t_i t_i \dots t_i$ that t_i has been fired many times continuously. Meanwhile, transition sequence t_7^*, t_8^*, t_9^* are compressed as (σ) , and the reachability graph of the compressed system model is shown in Fig. 5. The transition sequence between the markings in Fig. 5 is shown in Table III.

The original workflow will becomes an extended workflow when adding a new transition t_{16} in Fig. 3. If t_{16} is fired, the end marking will be transformed to the initial

TABLE 3
Transition sequences between the markings

$M_1 \rightarrow M_2$	$(t_1^* t_2^*) t_{10}$	$M_{12} \rightarrow M_{16}$	$t_5^* t_{13}$
$M_1 \rightarrow M_3$	$(t_2^* t_3^*) t_{11}$	$M_{12} \rightarrow M_{17}$	$(t_5^* t_6^*) t_{14}$
$M_1 \rightarrow M_4$	$(t_3^* t_4^*) t_{12}$	$M_{12} \rightarrow M_{18}$	(σ)
$M_1 \rightarrow M_5$	$(t_4^* t_5^*) t_{13}$	$M_{13} \rightarrow M_{16}$	t_{12}
$M_1 \rightarrow M_6$	$(t_5^* t_6^*) t_{14}$	$M_{13} \rightarrow M_{19}$	$t_6^* t_{14}$
$M_1 \rightarrow M_7$	(σ)	$M_{13} \rightarrow M_{20}$	(σ)
$M_2 \rightarrow M_8$	$t_3^* t_{11}$	$M_{14} \rightarrow M_{17}$	t_{12}
$M_2 \rightarrow M_9$	$(t_3^* t_4^*) t_{12}$	$M_{14} \rightarrow M_{21}$	$t_5^* t_{13}$
$M_2 \rightarrow M_{10}$	$(t_4^* t_5^*) t_{13}$	$M_{14} \rightarrow M_{22}$	(σ)
$M_2 \rightarrow M_{11}$	$(t_5^* t_6^*) t_{14}$	$M_{15} \rightarrow M_{23}$	$t_4^* t_{12}$
$M_8 \rightarrow M_{12}$	$t_4^* t_{12}$	$M_{15} \rightarrow M_{24}$	$(t_4^* t_5^*) t_{13}$
$M_8 \rightarrow M_{13}$	$(t_4^* t_5^*) t_{13}$	$M_{15} \rightarrow M_{25}$	$(t_5^* t_6^*) t_{14}$
$M_8 \rightarrow M_{14}$	$(t_5^* t_6^*) t_{14}$	$M_{16} \rightarrow M_{26}$	$t_6^* t_{14}$
$M_8 \rightarrow M_{15}$	(σ)	$M_{16} \rightarrow M_{27}$	(σ)
$M_{17} \rightarrow M_{26}$	t_{13}	$M_{24} \rightarrow M_{39}$	t_{12}
$M_{17} \rightarrow M_{28}$	(σ)	$M_{24} \rightarrow M_{40}$	$t_6^* t_{14}$
$M_{18} \rightarrow M_{29}$	$t_5^* t_{13}$	$M_{25} \rightarrow M_{41}$	t_{12}
$M_{18} \rightarrow M_{30}$	$t_6^* t_{14}$	$M_{25} \rightarrow M_{42}$	$t_5^* t_{13}$
$M_{19} \rightarrow M_{26}$	t_{12}		
$M_{19} \rightarrow M_{31}$	(σ)		
$M_{20} \rightarrow M_{32}$	t_{12}		
$M_{20} \rightarrow M_{33}$	$t_6^* t_{14}$		
$M_{21} \rightarrow M_{26}$	t_{12}		
$M_{21} \rightarrow M_{34}$	(σ)		
$M_{22} \rightarrow M_{35}$	t_{12}		
$M_{22} \rightarrow M_{36}$	$t_5^* t_{13}$		
$M_{23} \rightarrow M_{37}$	$t_5^* t_{13}$		
$M_{23} \rightarrow M_{38}$	$(t_5^* t_6^*) t_{14}$		

marking M_0 . Since $\forall t \in T$ and $\forall M \in R(M_0)$ are all $\exists M' \in R(M)$, $M'[t]$, the extended workflow with t_{16} is liveness. The rewritable edge such as (t_1, P_F) , (t_2, P_E) , (t_3, P_B) etc. will disappear, which depend on the number of collection times. The rewritable edge guarantees the boundedness of the places in the system framework model of rewritable petri net.

In summary, the extended work flow is liveness and boundedness through the analysis. Therefore, the system framework model are soundness.

4 OUR PROPOSED IUP SCHEME

In order to realize the utility prediction, we use deep learning to obtain the relationship between the parameters of the SSF process. To achieve sufficient data, this Section introduces the data generator model of MSE-GAN and the utility prediction model of SSF with fully connected networks.

4.1 The model of GAN

As introduced in the related work, we use GAN to generate more effective data to solve the few-shot problem. At the beginning of the training, keep the generator unchanged and then train the discriminator. Then, the generator and the discriminator play games. When the performance of generator is no longer improved, next, keep the discriminator unchanged and train the generator. The data generated

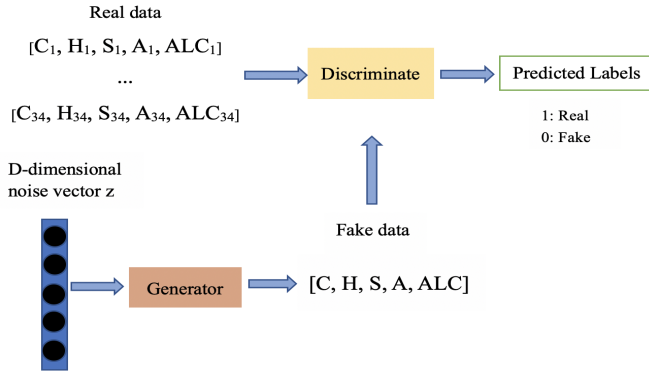


Fig. 6. The generation model of one-dimensional few-shot data based on GAN

by the generator, then the discriminator distinguish the real data and the data generated with the generator. Through the constant game between the discriminator and the generator. Finally, the discriminator cannot distinguish the real data and the generated data. The original GAN generate data algorithm is shown in [22].

4.2 The data generation model of few-shot one-dimensional based on MSE-GAN

The generator of MSE-GAN is a FCNN with four-layer, which input layer is five neurons. The output layer of generator has five neurons which is corresponding to the five categories of the generated one-dimensional data. The discriminator with three layers of fully connected network, which input is the one-dimensional data of five categories and the output is the data of 0 to 1 which represent the evaluation of whether the input data is real data. The network structure of generator and discriminator are shown in Fig. 7.

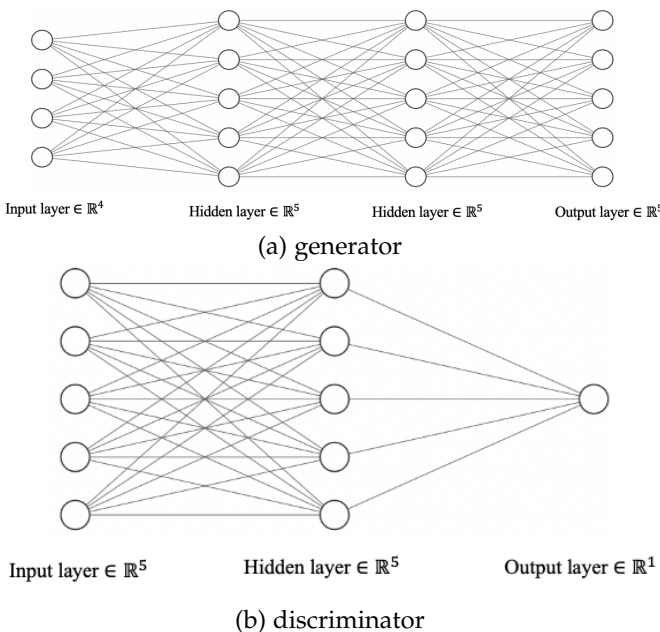


Fig. 7. The network structure of generator and discriminator

To avoid the large difference between the real data and generated data which is generated by the original GAN. We invent the algorithm of mean square error(MSE) with GAN to generate more effective one-dimensional data. The process is as follows, first, the real data is used as the input training data set, and then repeat training the 5 epochs by the model in Fig. 6, this step will generate amount data. Finally, making MSE between the generated data and the original data, as well as the generated data with a MSE greater than the threshold value are filtered out. The remaining data are retained as the appropriate generated data. The algorithm is as follows:

Algorithm 1: The algorithm of MSE-GAN

Input : Generated(original) data set; Real data set;

Output: Generated(final) data set;

- 1 **for** $data(g)$ in *Generated(original) data set* **do**
 - 2 **for** $data(r)$ in *real data set* **do**
 - 3 **if** *The MSE of $data(g)$ and $data(r) \leq$ threshold value* **then**
 - 4 Put the $data(g)$ into *Generated(final) data set*.
 - 5 Break.
 - 6 **end**
 - 7 **end**
 - 8 **end**
-

4.3 The utility prediction model for Chinese liquor SSF with fully connected neural network

This paper uses the FCNN to model the utility prediction of Chinese liquor SSF, the model is shown in Fig. 8. The main component of maternal draft is starch. Daqu is mainly composed of microorganisms. Bran shell provides more aerobic breathing space for microbial metabolism. Temperature is a necessary condition for SSF. As a result, the main parameters of SSF process are humidity, starch, acidity and temperature. These four parameters affect the quality and yield of alcohol. Therefore, firstly, we use temperature, humidity, starch and acidity as input vector, which dimension is 1×4 . Secondly, the input vector goes through the 4×64 dimensions, 64×128 dimensions, 128×256 dimensions and 256×128 dimensions orderly to explore the underlying connections between the input data. Finally, we can use a single neural getting one final value. The final production of alcohol value is activated by $\text{Tanh}(x)$ function which mitigate the problem of gradient disappearance. A batch normalization operation is added to ensure the stable of each output layer and reduce the phenomenon of gradient disappearance.

In this paper, we design the model of utility prediction for SSF, which includes learning algorithm and prediction algorithm.

Step 1: learning algorithm include 5 main input parameters Alcohol (*ALC*), cellar temperature (*C*), Humidity (*H*), Starch content (*S*), and Acidity (*A*). In the learning algorithm, we use the mean-square error as the loss function which is used to control the end of the loop and get the most accurate learning weight *W*. According to the gradient

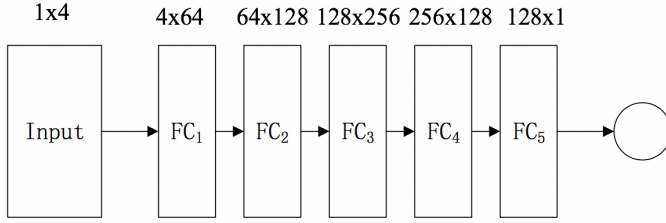


Fig. 8. A regression model with FCNN

descent function and the learning rate, the learning weight function W is obtained.

Step 2: according to the learning algorithm, The relationship model F_w is acquired. The model of F_w is a trained FCNN, which has been learned the relationships between parameters. Input the parameters of cellar temperature (C), Humidity (H), Starch content (S), and Acidity (A) into the model will get the target value Alcohol (ALC). These two algorithms are as follows.

Algorithm 2: The learning algorithm:.

Input:

$C, H, S, A, ALC;$

Output:

$W;$

- 1: **while** $Loss = (F(C, H, S, A) - ALC)^2 > \text{threshold do}$
 - 2: $\Delta \leftarrow -g((F(C, H, S, A) - ALC)^2)$ (Gradient descent)
 - 3: $W = W + \alpha \Delta$ (α is the learning rate)
 - 4: **end while**
 - 5: **return** $W;$
-

Algorithm 3: The prediction algorithm:.

Input:

$C, H, S, A;$

Output:

$ALC;$

- 1: $ALC \leftarrow F_w(C, H, S, A)$
(F_w is the relationship model of the process parameter)
 - 2: **return** $ALC;$
-

4.4 Data preprocessing

The data set is divided into training data set and test data set according to the ratio of 4:3. Partial SSF data are shown in Table IV. We can see that the range of values for each dimension attribute varies greatly. In order to accelerate the speed of network convergence, we adopt a min-max method to scale all the original data into $[0,1]$, the method is described as follows:

$$X = \frac{X - Min}{Max - Min}$$

5 PERFORMANCE ANALYSIS

In this Section, the accuracy of the prediction is tested and we compare our method with other prediction means. In

TABLE 4
The raw parameters of SSF

Cellar Temperature	Humidity%	Starch content%	Acidity%
40	45.31	35.17	1.42
40.5	45.4	34.85	1.55
43	45.4	34.25	1.69
42	45.42	34.12	1.69

addition, we also compare the predicted time with other methods

5.1 Experimental data generation

There are several parameters take effects on the process of liquor solid fermentation: temperature (C), humidity (H), starch (S) and acidity (A). We take them to be the main measurable attributes about the production of alcohol (ALC). Because other attributes of material carry out very limited influence to the alcohol, we will not take them into consideration. All of our experimental data come from the three wine cellars with similar environment A1, A2 and A3. We record J D B and E every two days and get 11, 11 and 12 groups of data from these wine cellars. Each pace of data is $1 * 5$ vectors.

First, we add some random factors to achieve the enhanced data, and put them into the original GAN to generate experimental data. However, the generated data differs greatly from the real data by original GAN. After that, we use the MSE-GAN to generate data under the same condition, which includes the same neural network and iterations. The data generated by the threshold value of 0.15 will be closer to the original data through several experiments. The results are shown in Fig. 9.

Fig. 9 presents the comparison of real data and generated data of 5 class which include C, H, S, A and ALC by MSE-GAN. we can see that the data generated by the MSE-GAN present a similar trend as the real data. Consequently, the data generated by MSE-GAN can be used for experimental analysis.

5.2 Comparison and analysis of experimental results

By the approach of MSE-GAN, we generated 1077 cases of data to train the FCNN to obtain the relationship between parameters. The model's structure is shown in Fig. 10, which is a FCNN model with one input layer, four hidden layers and an output layer. Input layer and each hidden layer includes 4 cells.

To compare the differences of the original GAN and the MSE-GAN, we use the data which generated by original GAN and MSE-GAN to train the alcohol prediction model of FCNN respectively, and use the 34 groups of real data to validate it. The results are shown in Fig. 11. The abscissa represents the sample number and the ordinate represents the alcohol concentration. The green line represents the original real alcohol concentration data, and the red line represents the alcohol concentration predicted by the trained FCNN after the generation of the original GAN model and MSE-GAN model respectively.

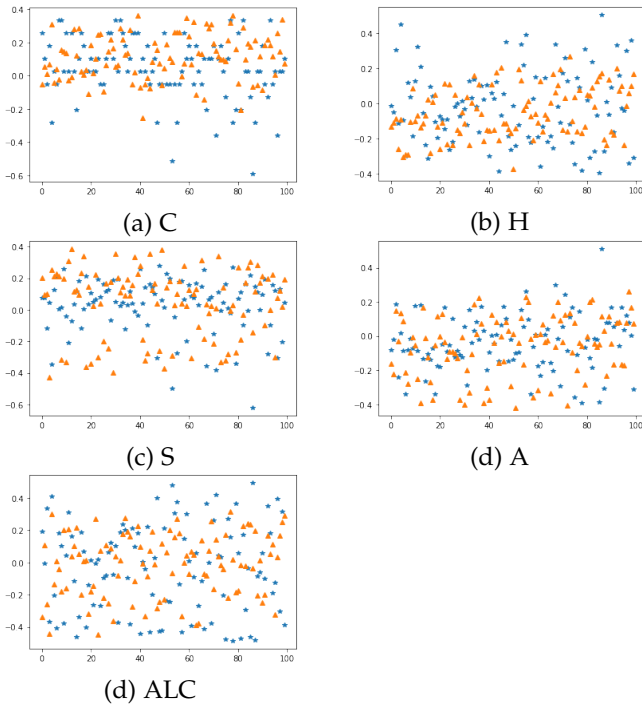


Fig. 9. The comparison of real data and data generated by MSE-GAN(real data: blue, generated data: orange)

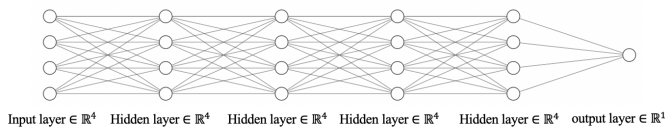


Fig. 10. The alcohol prediction model.

In this paper, we use the MSE to measure the effect of regression. The smaller the mean square error is, the more effective the regression prediction is. The MSE value of the data generated by the original GAN and MSE-GAN are 8.35 and 1.618 respectively, so the effect of data fitting which generated by original GAN is less than that generated by MSE-GAN.

In addition, we compare the method of FCNN with GAN prediction and the Multiple Linear Regression(MLR) by using the data which generated by the MSE-GAN. The prediction results are shown in Fig. 12, and the results of MSE are shown in Table V.

Moreover, we compare the prediction time of the three algorithms. We made the predictions for 34, 429, 750 and

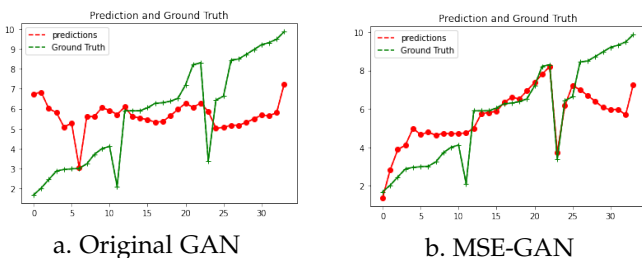


Fig. 11. FCNN prediction results of alcohol concentration based on the data generated by the Original-GAN and MSE-GAN

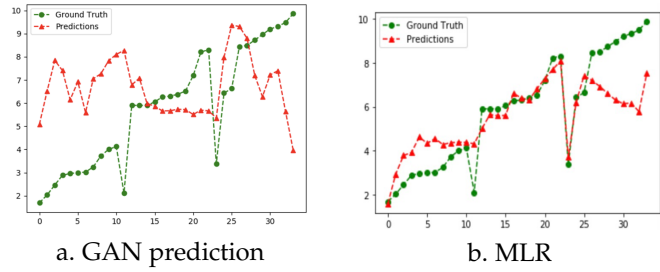


Fig. 12. The alcohol prediction results based on the prediction and MLR

TABLE 5
The mean-square error of three methods

Method	MSE
GAN prediction	9.128
MLR	2.167
FCNN	1.618

1,077 data sets, respectively. The time increment percentage of the three algorithms is shown in the Fig. 13.

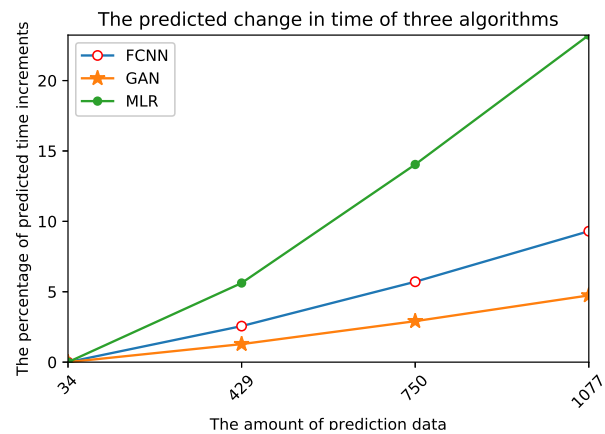


Fig. 13. The prediction time performance of three algorithms

It can be seen from the Table V that the MSE of FCNN is minimum, so FCNN is more effective than the other two methods. According to Fig. 13, we can see that the time change percentage of MLR is larger and the time change of GAN prediction is smaller. The difference of time change percentage between FCNN and GAN prediction is less than 5%.

In summary, the prediction accuracy and time performance of FCNN meet the expectations. This method can predict the quality and yield of SSF accurately in short time.

5.3 Engineering Application

SSF has a good application in food industry, enzyme preparation, organic acid flavor and other fields. SSF put the pre-proportion raw materials into the fermentation tank, and the fermentation process can not be controlled or changed any more. The production of liquor mainly relies on SSF. Fig. 14-15 shows the fermentation tank and digital management of a liquor SSF.



Fig. 14. The fermentation tank of liquor SSF

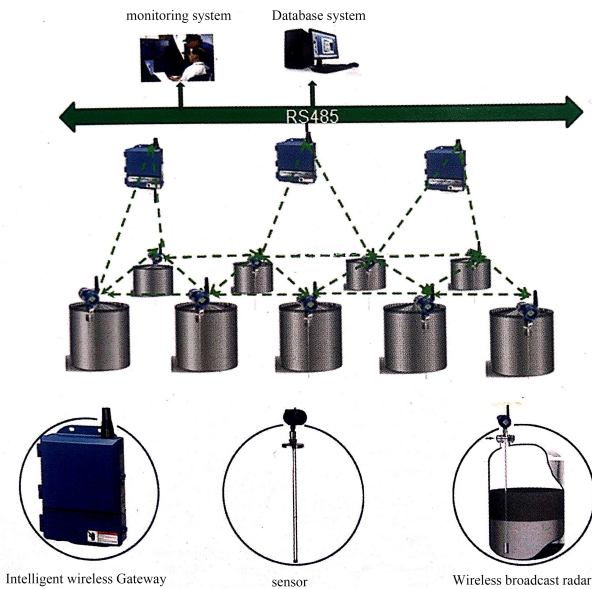


Fig. 15. The digital management of liquor SSF

However, the proportion of raw material depends on the artificial expertise, which would lead to the unstable yield and quality, as well as the waste of grain. To improve the utilization of grain in SSF, we can predict the quality and yield in advance according to the proportion of raw materials before SSF. In Fig. 16, we use deep learning to analyze the data of SSF collected in real time. Specifically, we use the improved GAN algorithm to generate the data when the collecting data is not enough. Then, the generated data and the actual data will be used as the training set by the FCNN for analyzing the relationship of these data. Finally, the yield and quality of SSF can be predicted according to the proportion of raw materials by FCNN.

We will focus on developing more efficient ways to adjust the proportion of raw materials according to the predicted quality and yield. In addition, the influence of microorganisms on SSF was not considered in this paper. In the future, the influence of microorganisms on SSF will be studied to further improve the utilization of grain.

6 CONCLUSION AND FUTURE WORK

We design a system for collecting parameters and predicting the quality and yield of liquor SSF in this paper. The system framework of liquor SSF was modeled by the edge-rewritable petri nets and the soundness of the model was

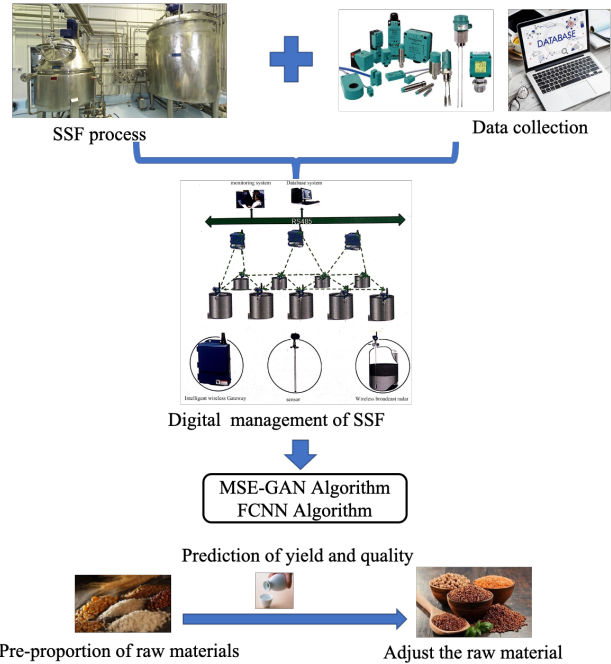


Fig. 16. The application of SSF prediction

proved. Because the data of SSF process is not enough, we proposed MSE-GAN to expand the original data as the training data. The relationship between the main parameters of the SSF process is analyzed by using the FCNN. Finally, the alcohol concentration can be effectively predicted according to the parameter of acidity, starch content, humidity and temperature. In this way, this paper provides data analysis for the ratio of preconditions and improves the yield and quality of liquor.

Since the effects of starch content, humidity, acidity and temperature on alcohol concentration were considered in this paper. However, microorganisms are another factors that affect the quality of SSF. In the future, we will study the quality of SSF by various microorganisms.

ACKNOWLEDGMENTS

This work was partially supported by the National Nature Science Foundation of China under Grant Nos.61572523, 61873281, 61672033, 61873280, and 61972416.

REFERENCES

- [1] R. R. Singhania, A. K. Patel, R. C. Soccol, "Recent advances in solid-state fermentation," *Biochemical Engineering Journal*, vol. 44, no. 1, pp. 13-18, Apr. 2009.
- [2] W. Zou, C. Q. Zhao, and H. Luo, "Diversity and Function of Microbial Community in Chinese Strong-Flavor Baijiu Ecosystem: A Review," *Frontiers in Microbiology*, vol. 9, no 671, pp. 1-15, Apr. 2018.
- [3] S. Rani, S. H. Ahmed, R. Rastogi, "Dynamic clustering approach based on wireless sensor networks genetic algorithm for IoT applications," *Wireless Networks*, vol. 26, no. 4, pp. 2307-2316, May. 2020.
- [4] X. N. Pang, B. Z. Han, X. N. Huang, X. Zhang, L. F. Hou, M. Cao, L. J. Gao, G. H. Hu, J. Y. Chen, "Effect of the environment microbiota on the flavour of light-flavour Baijiu during spontaneous fermentation," *Scientific Reports*, vol. 8, no. 1, pp. 3396, 2018.

- [5] X. Chen, K. Teng, H. Y. Hu *et al.*, "Production of Feng-Luzhou-flavor Combined Liquor by Strengthening Technical Research," *Liquor-Making*, vol. 35, no. 1, pp. 23-26, 2008.
- [6] L. J. Chai, P. X. Xu, W. Qian, "Profiling the Clostridia with butyrate-producing potential in the mud of Chinese liquor fermentation cellar," *International Journal of Food Microbiology*, no. 297, pp. 41-50, 2019.
- [7] X. N. Pang, X. N. Huang, J. Y. Chen, "Exploring the diversity and role of microbiota during material pretreatment of light-flavor Baijiu," *Food microbiology*, vol. 91, pp. 103514, Oct. 2020.
- [8] Y. Xuan, Yoshizaki, Yumiko, "Manufactural impact of the solid-state saccharification process in riceflavor baijiu production," *Journal of bioscience and bioengineering*, vol. 129, no. 3, pp. 315-321, Nov. 2019.
- [9] Z. L. Yi, Y. L. Jin, Y. Xiao, "Unraveling the Contribution of High Temperature Stage to Jiang-Flavor Daqu, a Liquor Starter for Production of Chinese Jiang-Flavor Baijiu," With Special Reference to Metatranscriptomics, *Frontiers in Microbiology*, vol. 10, no. 472, Mar. 2019.
- [10] Q. Li, Y. Gu, H. T. Wang, "The influence of temperature on flow-induced forces on quartz-crystal-microbalance sensors in a Chinese-liquor identification electronic-nose: three-dimensional computational fluid dynamics simulation and analysis," *APPLIED MATHEMATICS AND MECHANICS-ENGLISH EDITION*, vol. 40, no. 9, pp. 1301-1312, Sep. 2019.
- [11] S. Q. Xiang, Z. G. Zhang, "The Relations between the Production Factors in Solid-state Fermentation of Traditional Nongxiang Baijiu," *LIQUOR-MAKING SCIENCE & TECHNOLOGY*, no. 1, pp. 56-59, May. 2016.
- [12] T. Murata, "Petri nets: Properties, analysis and applications," *Proceedings of the IEEE*, Vol. 77, no. 4, pp. 541-580, 1989.
- [13] S. C. Pang, C. Lin, "Rewritable Petri Nets: Rewritable Place and Properties Analysis," *Chinese Journal of Computers*, vol. 35, no. 10, pp. 202-213, Oct. 2012.
- [14] Q. L. Lu, X. W. Xu, Y. Liu, I. Weber, W. Zhang, "uBaaS: A unified blockchain as a service platform," *Future Generation Computer Systems*. 2019.
- [15] Claudio Di Ciccio, Alessio Cecconi, Marlon Dumas, Luciano García-Bañuelos, Orleny Pintado, Qinghua Lu, Jan Mendling, Alexander Ponomarev, "Blockchain Support for Collaborative Business Processes," *Informatik Spektrum*. 2019.
- [16] C. Y. Yuan, "Principles and applications of Petri nets." *Electronic Industry Press*, pp. 23-56, Feb. 2005.
- [17] V. Rodriguez-Fernandez, A. Gonzalez-Pardo, D. Camacho, "Automatic procedure following evaluation using Petri net-based workflows," *IEEE Trans. Ind. Informat.*, vol. 14, no. 6, pp. 2748-2759, Dec. 2017.
- [18] Goodfellow, Ian and Pouget-Abadie, M. Mirza, X. Bing, Y. Bengio, "Generative Adversarial Nets," *In proc of the 2014 Conference on Advances in Neural Information processing System 27*. Montreal, Canada: Curran Associates, Inc, pp. 2672-2680, 2014.
- [19] I. Goodfellow. NIPS 2016 tutorial: generative adversarial networks. arXiv preprint arXiv: 1701.00160, 2016.
- [20] Y. Gao, R. Singh, B. Raj, "Voice Impersonation using Generative Adversarial Networks," 2018.
- [21] Y. Z. Zhang, Z. Gan, Lawrence Carin, "Generating text via adversarial training," *Workshop on Adversarial Training, NIPS 2016*, Barcelona, Spain, pp. 1-6, 2016.
- [22] T. N. Sainath, O. Vinyals, A. Senior, H. Sak, "Convolutional, Long Short-Term Memory, fully connected Deep Neural Networks," *IEEE International Conference on Acoustics*. IEEE, 2015.
- [23] J. Zhao, F. Deng, Y. Cai, J. Chen, "Long short-term memory - Fully connected (LSTM-FC) neural network for PM(2.5) concentration prediction," *Chemosphere*, no. 220, pp. 486-492, 2019.
- [24] Y. Wang, F. Zhang, X. Zhang, S. Zhang, "Series AC Arc Fault Detection Method Based on Hybrid Time and Frequency Analysis and Fully-connected Neural Network," *IEEE Transactions on Industrial Informatics*, pp. 1-10, Dec. 2018.
- [25] S. Y. Liu, H. Y. Guo, J. G. Hu, X. Zhao, M. Tang, "A novel data augmentation scheme for pedestrian detection with attribute preserving GAN," *Neurocomputing*, vol. 401, pp. 123-132, Feb. 2020.
- [26] F. Konidaris, T. Tagaris, M. Sdraka, A. Stafylopatis, "A Generative Adversarial Networks as an Advanced Data Augmentation Technique for MRI Data," *IEEE Trans Med Imaging*, vol. 37 no. 3, pp. 673-679, 2018.
- [27] Z. Liu, P. Qi, Y. Xu, H. Ma, G. Ren, "Misalignment calculation on off-axis telescope system via fully connected neural network," *IEEE Photonics*, pp. 1-14, 2020.
- [28] Y. Qi, C. Yu, C. X. Dai, "Research on Radar Plot Classification Based on Fully Connected Neural Network," *2019 3rd International Conference on Electronic Information Technology and Computer Engineering (EITCE)*. 2019.
- [29] H. Wang, H. Shi, K. Lin, A. CQ, B. LZ, A. YH, A. CL, "A high-precision arrhythmia classification method based on dual fully connected neural network," *Biomedical Signal Processing and Control*, vol. 58, pp. 101874, 2020.
- [30] F. Huang, J. Zhang, C. Zhou, Y. Wang, J. Huang, L. Zhu, "A deep learning algorithm using a fully connected sparse autoencoder neural network for landslide susceptibility prediction," *Landslides*, vol. 17, no. 1, pp. 217-229, 2020.
- [31] W. M. P. V. D Aalst, P. Barthelmeß, C. A. Ellis, J. Wainer, "Workflow Modeling using Proclefs," *International Conference on Cooperative Information Systems*. Springer-Verlag, 2000.
- [32] WMPVD. Aalst, AHMT. Hofstede, "YAWL: yet another workflow language," *Information Systems*, vol. 30, no. 4, pp. 245-275, 2005.
- [33] C. Lin, H. Khazaei, "Modeling and Optimization of Performance and Cost of Serverless Applications," *IEEE Transactions on Parallel and Distributed Systems*, pp. 615-632, 2020.
- [34] B. Sungho, A. Suh, C. PLB, OLA. Yong, "CEGAN: Classification Enhancement Generative Adversarial Networks for unraveling data imbalance problems," *Neural Networks*, vol. 133, pp. 69-86, 2021.
- [35] F. Liu, M. Xu, Li G, J. Pei, L. Shi, R. Zhao, "Adversarial symmetric GANs: Bridging adversarial samples and adversarial networks," *Neural Networks*, vol. 133, pp.148-156, Jan. 2020.
- [36] L. Yin, B. Zhang, "Time series generative adversarial network controller for long-term smart generation control of microgrids," *Applied Energy*, vol. 281, no. 116069, Jan 2021.
- [37] Noothout, M. H. Julia, De Vos, D. Bob, Wolterink, I. Igum, "Deep Learning-Based Regression and Classification for Automatic Landmark Localization in Medical Images," *IEEE transactions on medical imaging*, vol. 39, no. 12, pp. 4011-4022, Dec. 2020.
- [38] P. Huang, C. Wen, L. Fu, J. Lessan, X. Xu, "Modeling train operation as sequences: A study of delay prediction with operation and weather data," *Transportation Research Part E Logs and Transportation Review*, vol. 141, no. 102022, Sep. 2020.
- [39] X. Yu, H. Chen, M. Liang, Q. Xu, L. He, "A transfer learning-based novel fusion convolutional neural network for breast cancer histology classification," *Multimedia Tools and Applications*, pp. 1-15, Oct. 2020.
- [40] Y. Wang, S. Zhang, L. Yang, S. Yuan, T. Qin, "Measurement of Conditional Relatedness Between Genes Using Fully Convolutional Neural Network," *Frontiers in Genetics*, vol. 10, no. 1009, Oct. 2019.
- [41] L. Ale, N. Zhang, H. Wu, D. Chen, T. Han, "Online Proactive Caching in Mobile Edge Computing Using Bidirectional Deep Recurrent Neural Network," *IEEE Internet of Things Journal*, vol. 6, no. 3, pp. 5520-5530, Jun. 2019.
- [42] M. Ferreira, H. Fernandes, H. Peres, A. Oliva-Teles, I. Belo, JM. Salgado, "Bio-enrichment of oilseed cakes by *Mortierella alpina* under solid-state fermentation," *LWT- Food Science and Technology*, vol. 134, no. 109981, Dec, 2020.
- [43] Pourkhanali, Khadijeh; Khayati, Gholam; Mizani, Farhang; Raouf, Fereshteh, "Isolation identification and optimization of enhanced production of laccase from *Galactomyces geotrichum* under solid-state fermentation," *Preparative biochemistry & biotechnology*, pp. 1-10, Dec. 2020.
- [44] S. Saeed T. Mehmood, M. Irfan, "Statistical optimization of cultural parameters for the optimized production of alginate using apple (*Malus domestica*) peels through solid-state fermentation," *Biomass Conversion and Biorefinery*, Nov. 2020.
- [45] K Huang, Q Zhang, C Zhou, N Xiong, Y Qin, "An efficient intrusion detection approach for visual sensor networks based on traffic pattern learning," *IEEE Transactions on Systems, Man, and Cybernetics: Systems*, 47 (10), 2704-2713, 2017.
- [46] W Wu, N Xiong, C Wu, "Improved clustering algorithm based on energy consumption in wireless sensor networks," *IET Networks* 6 (3), 47-53, 2017.
- [47] Q Zhang, C Zhou, N Xiong, Y Qin, X Li, S Huang, "Multimodel-based incident prediction and risk assessment in dynamic cybersecurity protection for industrial control systems," *IEEE Transactions on Systems, Man, and Cybernetics: Systems* 46 (10), 1429-1444, 2015.

- [48] A Shahzad, M Lee, YK Lee, S Kim, N Xiong, JY Choi, Y Cho, " Real time MODBUS transmissions and cryptography security designs and enhancements of protocol sensitive information," *Symmetry* 7 (3), 1176-1210, 2015.
- [49] Y. Yang, N. Xiong, N.Y. Chong, X. Défago, " A decentralized and adaptive flocking algorithm for autonomous mobile robots," *The 3rd International Conference on Grid and Pervasive Computing*, 2008.